

AMERICAN UNIVERSITY OF BEIRUT

PCM COOLING VEST FOR IMPROVING COMFORT
UNDER HOT ENVIRONMENT

by
HANEEN IBRAHIM HAMDAN

A thesis
submitted in partial fulfillment of the requirements
for the degree of Master of Engineering
to the Department of Mechanical Engineering
of the Faculty of Engineering and Architecture
at the American University of Beirut

Beirut, Lebanon
May 2014

AMERICAN UNIVERSITY OF BEIRUT


PCM COOLING VEST FOR IMPROVING COMFORT
UNDER HOT ENVIRONMENT

by
HANEEN IBRAHIM HAMDAN


Approved by:


Prof. Nesreen Ghaddar PhD, Professor
Department of Mechanical Engineering

Advisor
May 16, 2014


Prof. Kamel AbouGhali, PhD, Professor
Department of Mechanical Engineering

Co-Advisor
May 16, 2014


Prof. Fadl Moukalled, PhD, Professor
Department of Mechanical Engineering

Member of Committee
May 16, 2014

Date of thesis defense: May 8, 2014

AMERICAN UNIVERSITY OF BEIRUT
THESIS, DISSERTATION, PROJECT RELEASE
FORM

Student Name: Hamdan Haneen Ibrahim
Last First Middle

Master's Thesis Master's Project Doctoral Dissertation

I authorize the American University of Beirut to: (a) reproduce hard or electronic copies of my thesis, dissertation, or project; (b) include such copies in the archives and digital repositories of the University; and (c) make freely available such copies to third parties for research or educational purposes.

I authorize the American University of Beirut, **three years after the date of submitting my thesis, dissertation, or project**, to: (a) reproduce hard or electronic copies of it; (b) include such copies in the archives and digital repositories of the University; and (c) make freely available such copies to third parties for research or educational purposes.

Haneen May 16, 2014
Signature Date

ACKNOWLEDGMENTS

I would like to express my sincere appreciation to my advisor Prof. Nesreen Ghaddar for her guidance, support, and advices on my research. I would like to thank her for encouraging my research and for allowing me to grow as a research scientist.

I would also like to thank my co-advisor Prof. Kamel Ghali for his support, guidance and brilliant comments and suggestions.

I would like to thank Prof. Fadel Moukalled as being a member of my thesis committee

I would also like to thank my parents and my friends for their constant support and motivation.

AN ABSTRACT OF THE THESIS OF

Haneen Ibrahim Hamdan for

Master of Engineering

Major: Mechanical engineering

Title: PCM Cooling Vest for Improving Thermal Comfort under Ho Environment.

This work investigates a passive method to extend cooling of the human body under hot environments for longer periods. A cooling vest containing phase change materials (PCM) made of salt mixtures that melts at a specific temperature helps in maintaining the skin temperature of the covered parts at a comfortable level. A transient mathematical model of heat and mass transfer through clothing layers containing PCM packets is developed. Two experiments were done on a clothed heated cylinder in a controlled environment to validate the proposed model. Good agreement was found between model-predicted and measured temperatures of the microclimate air between the cylinder and the PCM in both experiments. The PCM vest model is integrated with a segmental bio-heat model to provide realistic skin boundary conditions. The results from the integration were also validated with a published experiment on a human wearing a PCM vest subjected to hot environment. A simulation study on the different parameters affecting the performance of the vest is done. The parameters include the melting temperature, the covering area of the PCM and its mass. It was found that a lower melting temperature must be used when a fast cooling effect is desirable. Moreover, it is found that covering area is the factor that affects the cooling rate while the thickness or the mass of the PCM affect the cooling duration. These findings meet well with experimental conclusions of published data. The bio-heat model used divides the torso into eight different segments allowing studying the effect of the PCM on the upper and lower torso segments. It is found that the upper torso releases more sensible losses than the lower one when covered with the same number of PCMs.

CONTENTS

| | |
|----------------------|-----|
| ACKNOWLEDGMENTS..... | v |
| ABSTRACT..... | vi |
| NOMENCLATURE..... | ix |
| ILLUSTRATIONS..... | xi |
| TABLES..... | xii |

Chapter

| | | |
|------|---|----|
| I. | INTRODUCTION..... | 1 |
| | A. Introduction..... | 1 |
| | B. Methodology..... | 5 |
| II. | MODELING OF THE PCM COOLING VEST..... | 7 |
| | A. Mathematical Formulation..... | 7 |
| | 1. Fabric-PCM model..... | 7 |
| | 2. Microclimate and Macroclimate air modeling..... | 11 |
| | 3. Numerical Solution..... | 13 |
| | B. Results and Discussions..... | 13 |
| | 1. Model validation with experiments..... | 21 |
| | 2. Model validation with published data..... | 24 |
| III. | INTEGRATION OF THE MATHEMATICAL MODEL WITH THE SEGMENTAL BIOHEAT MODEL..... | 25 |
| | A. Introduction..... | 25 |
| | B. Validation of the integrated bio-heat model and the fabric-PCM model..... | 26 |

| | |
|--|----|
| C. Parametric Study using integrated bioheat model and fabric-PCM model..... | 29 |
| 1. Effect of PCM melting temperature..... | 29 |
| 2. Effect of the cooling vest covering area by the PCM..... | 32 |
| 3. Effect of the mass of the PCM..... | 33 |
| 4. Effect of the location of the PCM..... | 34 |
| IV. CONCLUSION..... | 40 |
| BIBLIOGRAPHY..... | 42 |

NOMENCLATURE

| | |
|---------------|--|
| A | area (m^2) |
| C_p | thermal capacitance ($J/kg \cdot K$) |
| e | thickness (m) |
| g | gravitational Acceleration (m/s^2) |
| h_{fg} | heat of Evaporation (J/kg) |
| h_{ad} | heat of Adsorption (J/kg) |
| h_{sf} | latent heat of fusion (J/kg) |
| h_m | mass transfer coefficient ($kg/m^2 \cdot kPa \cdot s$) |
| h_f | heat transfer coefficients ($kg/m^2 \cdot kPa \cdot s$) |
| h_c | convective heat transfer ($W/m^2 \cdot K$) |
| HD | hot dry |
| HH | hot humid |
| m | mass (kg) |
| \dot{m}_a | mass flow rate triggered by buoyancy forces |
| P | vapor Pressure (kPa) |
| R | Radius |
| R_d | dry Resistance of the fabric ($m^2 \cdot K/W$) |
| R_e | evaporative Resistance of the fabric ($m^2 \cdot kPa/W$) |
| R | fabric regain |
| w | humidity Ratio (kg_w/kg_{air}) |
| Greek Symbols | |
| α | Fraction of melted PCM |
| β | volumetric thermal expansion ($^{\circ}C^{-1}$) |

ρ density (kg/m^3)

ν kinematic viscosity of air (m^2/s)

Subscripts

air macroclimate air between the PCM and the environment

aj microclimate air between PCM and skin

env Environment

of outer fabric

if inner fabric

pcm Phase Change Material

ILLUSTRATIONS

| Figure | | Page |
|--------|--|------|
| 1 | Schematic of (a) side view of the skin and the different clothing, PCM, and air layers and (b) front and top view of the cooling vest in which PCM patches are placed on the upper and lower segments of the vests..... | 8 |
| 2 | Radii of different Layers..... | 10 |
| 3 | Schematic of (a-1) the clothed heated cylinder setup in the chamber and (a-2) the location of the thermocouples for Experiment1, (b-1) the clothed heated cylinder setup in the chamber and (b-2) the location of the thermocouples for Experiment2..... | 15 |
| 4 | Plots of the averaged experimental readings and the model predictions of (a) the microclimate air layer temperature and (b) the macroclimate air layer temperature during the melting phase..... | 19 |
| 5 | Plots of the averaged experimental readings and the model predictions of (a) the microclimate air layer temperatures adjacent to PCM(1) and PCM(2) and (b) the macroclimate air layer temperature during the melting phase..... | 21 |
| 6 | A plot of the variation in time of the PCM temperature in the published experiment [1] and the value predicted by the current fabric-PCM model..... | 23 |
| 7 | Flow chart of the integration of the fabric-PCM model with the Bio-heat Model..... | 25 |
| 8 | Plots of published experimental data [20] and the model predictions of (a) mean skin temperature and (b) rectal temperature for the case when PCM is present (PCM20) and for the case without the cooling device (CON)..... | 28 |
| 9 | A plot of the variation in time of the mean skin temperature of the torso for the base case without PCM and for PCM vest at three melting temperatures..... | 30 |
| 10 | A plot of the variation in time of the sensible heat loss of the torso for the base case without PCM and for PCM vest at three melting temperatures..... | 31 |

TABLES

| Table | | Page |
|-------|---|------|
| 1 | Comparison of Onset of melting, cooling duration and average sensible losses from torso during the melting phase between Vest21, Vest24 and Vest26..... | 32 |
| 2 | Comparison between 23% and 47% of PCM covering area of the torso | 33 |
| 3 | Comparison between two Vests of different Mass | 33 |
| 4 | Characteristic of different cooling vest cases..... | 34 |
| 5 | Comparison between the upper and the lower torso segments in different vest cases..... | 36 |

CHAPTER I

INTRODUCTION

A. Introduction

Workers in warm or hot environment are subject to higher thermal strain that affect their productivity and working endurance [1]. This is mainly due to the fact that the body will try to maintain its normal core temperature of 37 °C under these conditions by diverting blood the skin, rather than the muscles, in order to dissipate excess heat. If increased blood flow to the skin and the evaporative skin sweating are not enough to dissipate heat, the human core temperature will rise increasing the likelihood of thermal stress. Therefore, in order to increase working endurance in hot environment, passive cooling methods such as clothing ventilation and cooling vests have been used to combat heat stress [2].

In the last 15 years, research focused on design of personal cooling systems using blower fans, circulating liquid or phase change material (PCM) as a working microclimate medium [3- 7]. These systems can be found in the market with no clear optimized performance measures or predictive models to assess effectiveness in reducing thermal stress. Convection cooling systems are usually equipped with a blower or fan that forces air into the vest microclimate medium. This kind of system is moveable, quite inexpensive, but has a limited cooling capacity, high power consumption, and is ineffective in hot and humid weather [8]. Circulating liquid garments contain a pump that circulates cold liquid into small capillary tubes present in the vest. These garments have good heat removal capability for a relatively long duration. However, their heavy weight hinders the movement of the worker thus reducing

productivity [8]. Cooling vests with incorporated phase change materials (PCM), ice, paraffin or salt, are considered as the most promising techniques. Ice-based cooling vests were reported to help in reducing heat strain and in improving productivity under warm environments [9-11]. The main disadvantage of ice-based cooling vest is mainly in the very low melting temperature that may cause erythema and thus discomfort [12]. The salt PCM is superior to ice since it can be incorporated in the fabric structure in microcapsules or used as packs with the possibility of controlling the melting temperature. There is a large variety of PCMs that are characterized by their non-toxicity, high melting temperatures and large latent heat of fusion [13]. The incorporation of PCM microcapsules in the fabric was not very successful due to volume and heat capacity constraint and inability to regenerate itself by ventilation in warm climates [14] and researchers have focused on the salt packs to find the optimum design of cooling vest that suits a specified work and does not affect the wearer's mobility [15-19].

Chou et al. investigated empirically the relationship between clothing property factors, physiological effects, and techniques of lessening physiological strain to improve performance of firefighters [20]. They studied mainly the PCM and ICE (ice-packs) techniques and concluded that PCMs are more efficient than ICE because of their large surface cooling area, higher melting temperature, and softer material [20]. Reinertsen et al. studied experimentally the performance of PCM material and the effect of its position on thermal comfort and sensation under simulated work situations [21]. Experiments were done on people wearing well-insulated clothing in a hot environment. The effects of cooling elements covering the whole trunk or the upper trunk were compared. The results showed that although the skin temperature remained lower when the whole trunk is covered, the reduction in thermal stress was better when the upper trunk is covered due to less sweat produced.

In another study by Bendkowska et al. [22], a thermal manikin was used with skin temperature set at 34 °C to investigate the cooling effect of a PCM cooling vest to be worn under chemical protective garments at ambient air of 20°C. Macro PCMs were inserted in small packs and placed on the inner surface of the vest near the skin. Their results showed that vest melting temperature and low initial temperature provide best performance. Other findings by Gao et al [23] showed that the cooling effect depended on surface temperature of the manikin as well as the melting temperature of the PCM. Human subjects experiments showed that while performing cycling under hot environments, the chest skin temperature and the mean skin temperature increased but remained lower by about 3-5 °C when wearing the PCM vest [23]. An empirical correlation by Gao et al. [1] has been derived for the PCM cooling effect and temperature gradient between skin and PCM melting point, mass of PCM, and the covering area using three types of PCMs with different melting points (24 °C, 28 °C, and 32 °C). Experiments done on human subjects [24] validated the findings of the previous work [1] and showed that lower the melting temperature the stronger is the cooling effect on the torso and the mean skin temperature [24]. The efficiency of the PCM cooling vest in hot humid (HH) and hot dry (HD) environments was also compared by Zhao et al. [25]. They showed that the cooling vest is effective only in the HH case.

In addition to experimentation, the effect of wearing a vest with PCM was also studied numerically using a simple human thermoregulation model to predict the surface heat flow [26]. In order to find the inner surface temperature of the PCM, they developed a mathematical model based on enthalpy balance and the model compared well with some published experimental results on skin and core temperature [26]. Ghali et al. performed a numerical study along with experiments to investigate the transient effect of a microencapsulated PCM-fabric subject to

periodic ventilation [14]. They reported that the PCMs helped in delaying the transient response when the fabric is subjected to sudden change in environmental conditions but the PCM was unable to regenerate itself under ventilated conditions.

The previous work on assessing performance of PCM vests has focused on empirical methods and the few modeling studies of cooling vests have only addressed uniform PCM material at fixed melting temperature. Some of the drawbacks of use of PCM salt packages in cooling vests are their weight and limited duration. There is a need to optimize the design of the vest making its weight lighter without jeopardizing the duration of its applicability and taking into consideration the existence of more sensitive trunk regions to cooling comfort. There is room for reducing the weight of the PCM by considering PCM placement location for better human local thermal response. Major performance parameters for optimization of the PCM vest design can include location of PCM and having non uniform melting point with non-uniform weight when distributing the packages of PCM over the upper body. The current literature modeling techniques cannot be used to effectively design the new vest and incorporate in the modeling non-uniformity of melting as well as the weight of the salt packages. The new idea in this study is having non uniform packages in terms of melting point temperature and weight arranged inside the same cooling vest. We believe that the study will help in achieving the alleviation of thermal stress of workers at a lower weight of cooling vest and better comfort conditions. A responsive segmental bio-heat model integrated with versatile PCM model would result in an important optimization tool that can be developed to determine best design that maintains stable core temperature for the longest period.

The aim of this work is to introduce enhancements to the PCM cooling vest design and use human body modeling tools to enable studying interventions that improve productivity in hot

environment while correlating it to worker physiological thermal states. A new simplified model will be developed of the PCM cooling vest as well as clothing microclimate inner air layer. The PCM cooling vest model will then be integrated with a segmental bioheat model to predict the skin temperature, which is used as boundary condition for the PCM cooling vest model [2, 27-28]. The PCM cooling vest model will be validated by experiments in a controlled chamber using constant flux heated cylinder while the integrated PCM vest and bioheat model will be validated with published experimental data. A parametric study is then performed to obtain the effect of the different PCM design parameters in improving the PCM cooling vest effectiveness and recommend optimal designs.

B. Methodology

In this work, a dynamic thermal model is developed for a PCM cooling vest to simulate heat and mass transfer through the clothing layers with PCM packets integrated within the air layers. The model predicts the temperature and the moisture content of the different fabric layers and the associated air gaps between them at given ambient conditions and for a given skin temperature and known number of PCM packets and their thermophysical properties along with the type of clothing and their dry and evaporative resistances. The fabric-PCM model is then be integrated with a multi-node segmental and transient bio-heat model capable of predicting accurately the segmental skin and core temperature of all body segments [27-28]. The skin temperature obtained from the bioheat model will be used in the fabric-PCM model such that both continuity of flux and skin temperature are observed at each time step. Thus the skin and the core temperatures of these segments will depend on the microclimate air temperature calculated by the fabric-PCM model.

The fabric-PCM model is validated with experiments performed on a clothed heated cylinder in a controlled chamber to compare predicted and measured air temperatures of the air gaps trapped between the different layers at different conditions. The model predicted temperature transient of the PCM is also validated with published experimental data. In addition, the integrated fabric-PCM model and bioheat model will also be validated with published experimental data on human subjects wearing PCM cooling vest.

The validated fabric-PCM model and bioheat model will be then be used as an optimization tool for the vest design based on performance. A parametric study is performed on different parameters affecting the performance of the vest to offer recommendations for improved design.

CHAPTER II

MODELING OF PCM COOLING VEST

A. Mathematical Formulation

To mathematically model the effect of varying the location, weight and melting point temperature of the PCM materials on the microclimate temperature of the clothing system as well as the corresponding physiological responses of the worker wearing the cooling vest this would require a fabric-PCM heat and moisture transport model, and a detailed human segmental human body model. The segmental bio-heat model will constitute a boundary condition for the fabric-PCM model.

1. Fabric-PCM Model

The worker is assumed to wear the PCM cooling vest over a thin underclothing layer. The vest is made of a low evaporative resistance fabric to facilitate moisture transfer to the environment and it contains pockets to hold the PCM packs. Figure 1 depicts schematic of (a) side view of the skin and the different clothing, PCM, and air layers and (b) front view of the cooling vest in which PCM packets are placed on the upper and lower segments of the vests. The thin inner layer of cotton is necessary for preventing any direct contact of the PCM with the skin. Above this layer is the inner air layer followed by the distributed PCM material of known quantity and known melting point temperature. The PCM is then covered by an outer protective fabric layer. There is also an air layer separating the PCM and the outer fabric. For this

arrangement, the PCM packet material is hanging between the inner and outer layers without being bonded to either layer but it is closer to the underlying layer because of the Velcro fasteners. In such a case, the phase change material directly affects the temperature of the trapped air layer between the inner underlying layer and the PCM packet while allowing vertical buoyancy motion in this thin trapped inner air layer adjacent to the PCM.

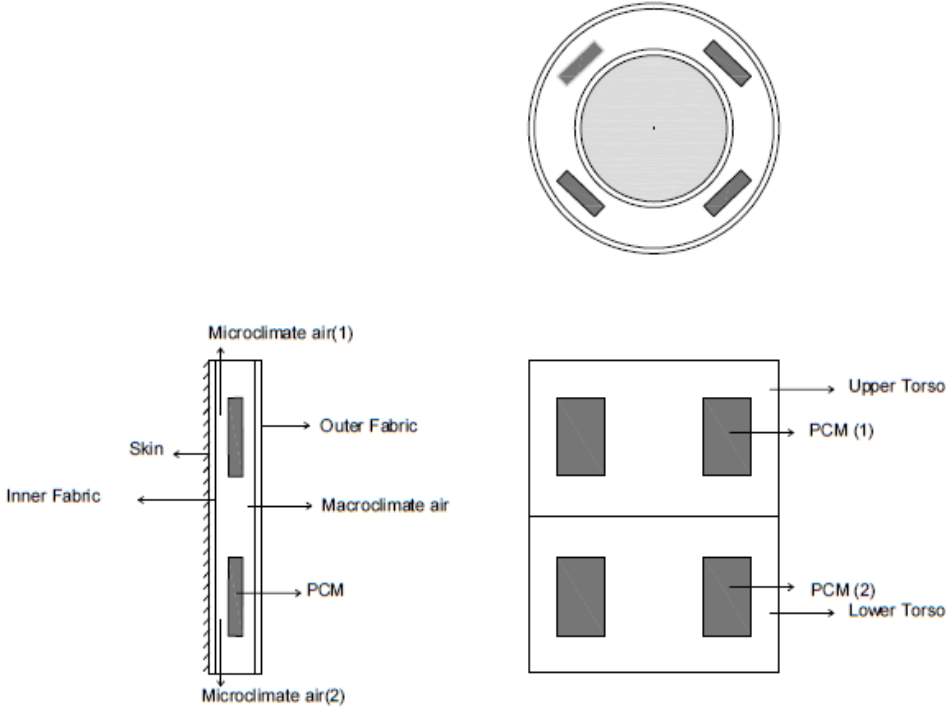


Figure 1: Schematic of (a) side view of the skin and the different clothing, *PCM*, and air layers and (b) front and top view of the cooling vest in which *PCM* patches are placed on the upper and lower segments of the vests

Prior to wearing the vest, the *PCM* is assumed to be solid. In work conditions, the heat and moisture from the body surface is transferred to the microclimate air whose temperature depends on the amount of the transported heat and the enclosed *PCM* material. The macro

climate air temperature is modeled as lumped air layer with a uniform temperature T_{air} between the PCM packets and behind the packets as shown in the Fig. 1. In the regions between the PCM packets and the underlying clothing, the microclimate temperature is different than the surrounding macroclimate air since Velcro fasteners are used to bring the PCM material closer to the body.

Mass and energy balance equations for heat and mass transport are written for each fabric and PCM layer. The underlying clothing layer exchanges heat and water vapor transfer with the skin and the microclimate air layer. The regions of microclimate air layer between each PCM piece and the underclothing layer is taken to be lumped. However, each region has its own conditions depending on the PCM melting temperature and its position. On the other hand, the macroclimate air layer along the vest is basically at a lumped air temperature.

The Mass and energy balances for the underlying fabric layer are respectively given by

$$\rho_{if} * e_{if} * \frac{dR_{if}}{dt} = \frac{P_{skin} - P_{if}}{\frac{R_{e,if} * h_{fg}}{2} + \frac{1}{2 * h_m}} + \frac{A_f - \sum A_{pcmj}}{A_f} * \frac{P_{air} - P_{if}}{\frac{R_{e,if} * h_{fg}}{2} + \frac{1}{2h_m}} + \frac{\sum A_{pcmj}}{A_f} * \frac{P_{aj} - P_{if}}{\frac{R_{e,if} * h_{fg}}{2} + \frac{1}{2h_m}} \quad (1)$$

$$\rho_{if} * e_{if} * (C \frac{dT_{if}}{dt} - h_{ad} \frac{dR_{if}}{dt}) = \frac{T_{skin} - T_{if}}{\frac{R_{d,if}}{2} + \frac{1}{2h_f}} + \frac{A_f - \sum A_{pcmj}}{A_f} * \frac{T_{air} - T_{if}}{\frac{R_{d,if}}{2} + \frac{1}{2h_f}} + \frac{\sum A_{pcmj}}{A_f} * \frac{T_{aj} - T_{if}}{\frac{R_{d,if}}{2} + \frac{1}{2h_f}} \quad (2)$$

Where T_{if} is the inner fabric temperature, T_{air} is the temperature of the air layer (macroclimate air) sandwiched between the outer fabric, the PCM, and the inner fabric as shown in Fig. 1, T_{aj} is the air temperature trapped between the PCM and inner fabric, A_f is the fabric area, $R_{d,if}$ is the inner fabric dry resistance, C is the inner fabric capacitance, e_{if} is the inner fabric thickness, R_{if} is the fabric regain, P is the vapor pressure, h_{fg} is the heat of evaporation, $R_{e,if}$ is the fabric evaporative resistance, h_m is the mass transfer coefficient of inner fabric ($kg/m^2 \cdot kPa \cdot s$), h_f is the heat transfer coefficients of inner fabric ($kg/m^2 \cdot kPa \cdot s$), h_{ad} is heat of

adsorption of the fabric, h_c , is the convective heat transfer of the inner air enclosed between the inner and outer fabrics, $A_{pcm,j}$ is the surface area of the PCM packet and n is the number of PCM packets distributed inside the cooling vest.

When there is no phase change ($T_{pcm} < T_{pcm}$ PCM melting temperature), the PCM is treated as a dry intermediate layer and its energy equation is then similar to fabric layer equations as follows:

$$m_{pcmj} * C_{pcmj} * \frac{dT_{pcmj}}{dt} = h_c * A_{pcmj} * (T_{aj} - T_{pcm}) \frac{r_{if}}{r_{pcm}} + h_c * A_{pcmj} * (T_{air} - T_{pcm}) \quad (3)$$

The ratio r_{if}/r_{pcm} takes into account the increase in the resistance due to difference in the areas of the different layers due to the cylindrical geometry as reported in Ref [29]. This ratio is close to unity for small gap width. Figure 2 shows the radii of the different layers.

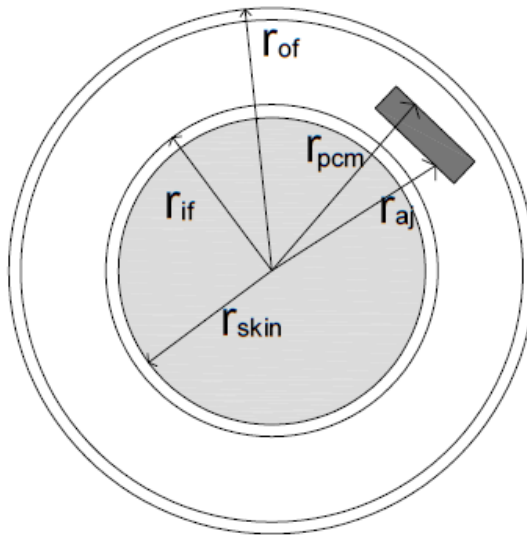


Figure 2: Radii of different Layers

During the phase change, $T_{pcm} = \text{constant}$ and it is equal to the PCM melting temperature and the heat transport equation is given by

$$h\text{-sf} * m_{pcm} * \frac{da_j}{dt} = h_c * A_{pcm} * (T_{aj} - T_{pcm}) * \frac{r_{if}}{r_{pcm}} + h_c * A_{pcm} * (T_{air} - T_{pcm}) \quad (4)$$

The mass and energy balances for the outer fabric layer are respectively given by

$$\rho_{of} * e_{of} * \frac{dR_{of}}{dt} = \frac{P_{env} - P_{of}}{\frac{R_{e,of} * h_{fg}}{2} + \frac{1}{2h_m}} + \frac{P_{air} - P_{oif}}{\frac{R_{e,of} * h_{fg}}{2} + \frac{1}{2h_m}} \frac{r_{if}}{r_{of}} \quad (5)$$

$$\rho_{of} * e_{of} * (C \frac{dT_{of}}{dt} - h_{ad} \frac{dR_{of}}{dt}) = \frac{T_{env} - T_{of}}{\frac{R_{d,of}}{2} + \frac{1}{2h_f}} + \frac{T_{air} - T_{of}}{\frac{R_{d,of}}{2} + \frac{1}{2h_f}} \frac{r_{if}}{r_{of}} \quad (6)$$

where T_{env} is the environment temperature, T_{of} is the outer fabric temperature, $R_{d,of}$ is the outer fabric dry resistance, C is the outer fabric capacitance, e_{of} is the outer fabric thickness, R_{of} is the outer fabric regain, $R_{e,of}$ is the outer fabric evaporative resistance, h_m is the mass transfer coefficient of the outer fabric ($\text{kg/m}^2 \cdot \text{kPa} \cdot \text{s}$), h_f is the heat transfer coefficients of the outer fabric ($\text{kg/m}^2 \cdot \text{kPa} \cdot \text{s}$).

2. Microclimate and Macroclimate Air Modeling

Assuming that the gap width between the PCM pack and the underlying clothing layer to be small, the air flow in this region that is triggered by buoyancy forces caused by temperature differences and can be assumed to follow the Poiseuille flow regime due to the small gap width.

The mass flow rate of air is represented by Bejan [30] as:

$$\dot{m}_a = \rho_{air} * g * \beta * \frac{T_{air} - T_{aj}}{12\nu} * d^3 * w \quad (7)$$

where ρ_{air} is the density of air, g is the gravitational acceleration, β is the thermal expansion of air, d is the gap width, w is the width of the PCM packet, ν is the kinematic viscosity of air.

The mass and energy balances for microclimate air are respectively given be

$$\rho_{air} * d * \frac{dw_{aj}}{dt} = \sum \frac{P_{if} - P_{aj}}{\frac{R_{e,*} * h_{fg}}{2} + \frac{1}{2h_m}} \frac{r_{if}}{r_{aj}} + \dot{m}_a * (w_{air} - w_{aj}) * \frac{1}{d * w} \quad (8)$$

$$\rho_{air} * d * A_{pcn,j} * C \frac{dT_{aj}}{dt} = A_{pcmj} * h_c * (T_{pcm} - T_{aj}) + A_{pcmj} * h_c * (T_{if} - T_{aj}) \frac{r_{if}}{r_{aj}} + \dot{m}_a * C_{air} * (T_{air} - T_{aj}) \quad (9)$$

The mass and energy balances for macroclimate air are respectively given be

$$\rho_{air} * e_{air} * \frac{dw_{air}}{dt} = \frac{P_{of} - P_{air}}{\frac{R_{e,*} * h_{fg}}{2} + \frac{1}{2h_m}} \sum \dot{m}_a * (w_{aj} - w_{air}) * \frac{1}{d * w} + \frac{A_f - \sum A_{pcmj}}{A_f} * \frac{P_{if} - P_{air}}{\frac{R_{e,*} * h_{fg}}{2} + \frac{1}{2h_m}} \frac{r_{if}}{r_{air}} \quad (10)$$

$$\begin{aligned} \rho_{air} * e_{air} * (C * \frac{dT_{air}}{dt} - h_{fg} * \frac{dw_{air}}{dt}) &= h_c * (T_{of} - T_{air}) + \sum \frac{A_{pcmj}}{A_f} * h_c * (T_{pcmj} - T_{air}) \\ &+ \frac{A_f - \sum A_{pcmj}}{A_f} * h_c * (T_{if} - T_{air}) + h_{fg} * \frac{P_{of} - P_{air}}{\frac{R_{e,*} * h_{fg}}{2} + \frac{1}{2h_m}} \\ &+ h_{fg} * \frac{A_f - \sum A_{pcmj}}{A_f} * \frac{P_{if} - P_{air}}{\frac{R_{e,*} * h_{fg}}{2} + \frac{1}{2h_m}} \frac{r_{if}}{r_{air}} + \sum \dot{m}_a * C_{air} * (T_{air} - T_{aj}) \end{aligned} \quad (11)$$

To solve the above coupled equations, initial conditions for all clothing layers and PCM are needed. The skin temperature is either assumed isothermal when testing the PCM vest model independently on a clothed cylinder or from integration with the bioheat model [28]. The fabric regain must be known initially and it can be evaluated from the fabric regain correlation to relative humidity of the environment [31]. A first order numerical model will be developed using standard numerical integration techniques.

3. Numerical solution

The above equations will be solved algebraically using the explicit Euler forward method providing the initial conditions such as the temperature and the pressure of all the

different layers of clothing and air, as well as the initial PCM temperature. Initially the air layers, inner and outer fabric are considered to be at equilibrium with environment. First, the regain of the inner and outer fabrics at time $t+\Delta t$ will be calculated using equations (1) and (5) respectively. Thus, the temperatures of the inner and outer fabrics at $t+\Delta t$ can now be calculated using equations (2) and (6) respectively. Using the interpolation function of regain versus relative humidity of fabric [31], which is a fabric property, the relative humidity of the fabrics can be calculated. At the same time, the saturation pressure of the fabrics at the previously calculated temperatures can be calculated at $t+\Delta t$ using psychometric formulas of Hyland and Wexler [32]. Therefore, the vapor pressures of the fabrics at $t+\Delta t$ step can be found.

For the microclimate and the macroclimate air layers, the humidity ratios and the temperatures at the new time $t+\Delta t$ are found after calculating the air flow rate due to buoyancy in the different microclimate layers using equation (7). For the updated temperature evaluation of the PCMs, at each time step, they are compared against the PCM melting temperature and accordingly, either the temperature at the $t+\Delta t$ is calculated from the single phase equation (3), or kept constant while the PCM melted fraction α , is calculated during change of phase (melting) using equation (4).

B. Results and Discussions

1. Model validation with experiments

The aim of the experiments is to validate the fabric-PCM model predictions of lumped temperatures of the microclimate air layer (adjacent to human body) and the macroclimate air layer (adjacent to environment) during the melting phase and to test the ability of the fabric-PCM model in handling two non-uniform microclimate environments and predicting accurately their

associated temperatures. The PCM material used in our tests is made of a non-toxic, non-flammable salt mixture sealed inside an aluminum wrapper. It is mainly made of sodium sulfate and water called Gaulber's salt [1]. The melting temperature of the PCM used in the experiments is 28°C. The latent heat of fusion is 126 kJ/kg and the specific heat is 3.6 kJ/kg. The material's density is 1.45 kg/m³ [33]. The dimensions of the PCM packet used are 13 cm height × 7 cm width × 1 cm thickness.

Two experiments were conducted on a clothed heated cylinder placed in a controlled climatic chamber set at 28 ± 0.5 °C and relative humidity of $50 \pm 2\%$ [34]. Three concentric metallic mesh cages placed around the heated cylinder are used to hold the PCM packets and the fabric. The first experiment used single uniform PCM packet at initial temperature lower than the environment and inserted between a heated cylinder and the fabric. The second experiment used two identical PCM packets inserted at different locations of clothed heated cylinder and at different initial temperatures to examine effectiveness of the model with different PCM arrangement on the clothed cylinder. Figure 3 shows the schematic of the clothed heated cylinder experimental setups and other components of (a-1) experiment one and (b-1) experiment two respectively. The clothed cylinder consists of: (i) a copper hollow inner cylinder with a diameter of 0.104 m and a length of 0.215 m; (ii) two thin metallic screens of 2 cm open squares of 0.215 m in length and 0.108m and 0.128 m diameters respectively to hold the PCM packets; (iii) an outer fabric of 0.215 m long and 0.14 m diameter metallic mesh cylinder; (iv) support platform; (v) Styrofoam insulative material to insulate the bottom of the vertical cylinder. The concentric cylinders are fixed at the lower end to the supporting insulated frame. The cotton fabric used in the two experiments was obtained from Test fabrics Inc. (Middlesex, NJ 08846), and is made of unmercerized cotton duck, style #466 of thickness of 1 mm and permeability of

0.05 m³/m²•s. The heated cylinder is wrapped with metallic resistance heaters Omega-KH-1012 to produce constant heat flux condition per heater at the cylinder surface. In both experiments, the heat fluxes from the heaters are regulated independently such that an almost uniform mean steady temperature of 35 °C ±0.5 °C is attained for each strip heater due the high conductivity of the surface heaters.

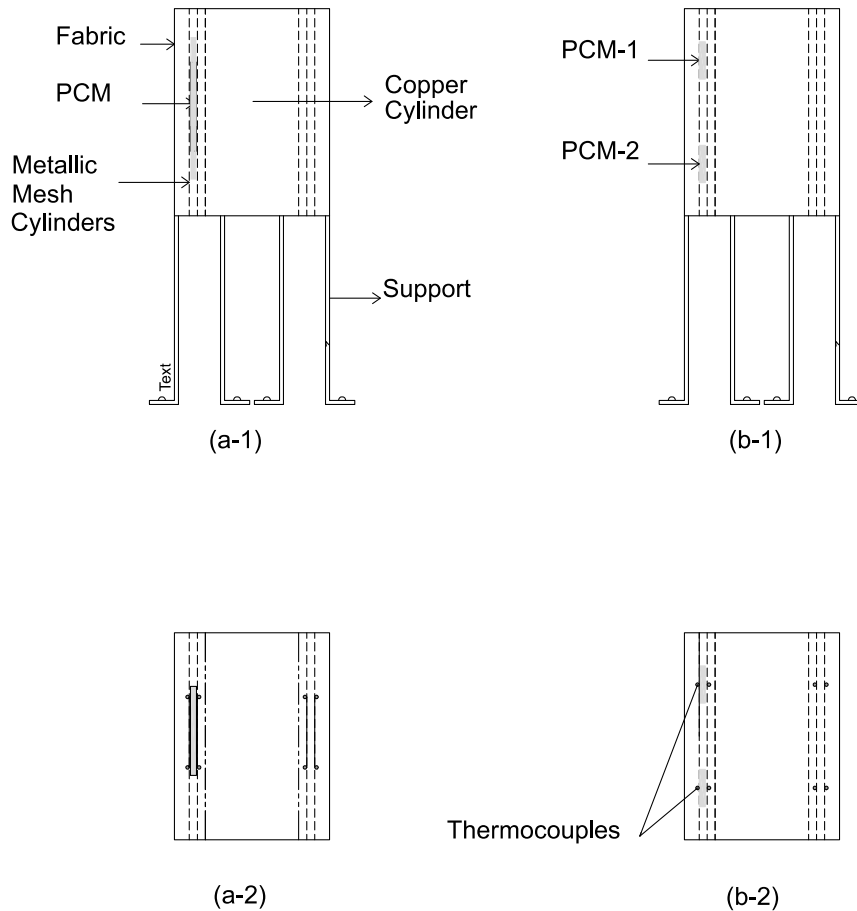


Figure 3: Schematic of (a-1) the clothed heated cylinder setup in the chamber and (a-2) the location of the thermocouples for Experiment1, (b-1) the clothed heated cylinder setup in the chamber and (b-2) the location of the thermocouples for Experiment2

The configuration of the clothed cylinder allowed the formation of two air layers, the microclimate air confined between the PCM packet and the heated cylinder and the

macroclimate air confined between the PCM packet and the fabric. The temperature of each air layer is measured by two thermocouples mounted on the mesh cages at two positions in the region adjacent to the PCM packet as shown in figure 3 (a-2). The three metallic cages holding the PCM packet and the outer fabric were held tight before placing them around the heated cylinder. The thermocouples were also placed in their appropriate position on the cages.

In the first experiment, one PCM packet of the dimensions 13 cm height \times 7 cm width \times 1 cm thickness was kept at 20°C to solidify all night in a climatic room in an open wooden box. At first, the heated cylinder was kept for 10 minutes to reach the desired steady surface temperature, and then the PCM packets at 20°C was brought from the conditioned 20°C in its wooden box which was covered by a lid into the experimental climatic room and immediately taken out of the box and placed in the designated location around the cylinder. This step took one minute while the data is being logged. At the onset of the experiment, the PCM temperature was 21°C. The average value of the two thermocouple readings of the air layer temperature is compared against the predicted one. The thermocouple readings, the climatic chamber conditions were monitored in time by a data acquisition system of national instruments SCXI 1121, and Labview software. The temperatures were sampled at 10 reading/s and are averaged and recorded every 60 seconds with an accuracy of $\pm 0.1^\circ\text{C}$.

In the second experiment, two identical PCM packets were used, (PCM-1) and (PCM-2) with dimensions of 7 cm height \times 7 cm width \times 1 cm thickness each. The two PCM packets were placed consecutively with a 7.5 cm distance between them. This configuration allows the formation of a microclimate air layer behind each of the two PCM packets. The temperatures of these two air layers were measured by thermocouples mounted on the mesh cages in the appropriate position as shown in figure 3 (b-2). Similarly, two thermocouples were used to

measure the temperature of the macroclimate air layer. The two PCMs were kept all night to solidify at two different temperatures, one at 11 °C and the other PCM at 20°C. Similar to the protocol of the first experiment, the two PCMs were inserted in their appropriate locations directly after the heated cylinder reached the desired temperature. At the onset of the experiment, the initial temperatures of the two PCM packets were measured using “Laser-Gun” thermometer. The initial temperature of (PCM-1) was 11.7°C while that of (PCM-2) was 20.5°C. The readings of the thermocouples were recorded by the same data acquisition system used in the first experiment.

This section compares the experimental results against those predicted by the fabric-PCM model. In each case, the clothed heated cylinder with the PCM geometry was simulated at the same experimental environment temperature to compare the temperature values of micro- and macro- climate air predicted by the model and values recorded in the experiments. Figure 4 shows the averaged experimental readings and the model predictions of (a) the microclimate air layer temperature and (b) the macroclimate air layer air layer temperature during the melting phase. A good agreement is found in general between the measured and predicted values of micro and macro climate air temperatures. Examining the microclimate air, which resembles the air gap between the PCM and the heated cylinder, the maximum error was found to be about $\pm 4.5\%$, corresponding to 1.1°C. However, the maximum error for the macroclimate air, which is the air trapped between the PCM and the outer fabric exposed to the environment, was around 2.5% during the melting phase which corresponded to $\pm 0.5^\circ\text{C}$. The errors are easily explained by the lumping assumption of the PCM and the consideration of a uniform temperature at all positions throughout the melting phase when the PCM reaches melting point. In real applications, the inner surface of the PCM melts first. Therefore, in the

microclimate air, the experimental value of temperature was lower than the predicted one because the melting at the inner surface of the PCM in the experiment started before the predicted one by the model which assumes uniform temperature across the whole mass. As the melting process continued, the experimental temperature of the microclimate air did not show the slight decrease similar to the predicted values because of the slight increase of the PCM inner surface facing the heated skin. On the other hand, the experimental values of the macroclimate air temperature was greater than that of the predicted one by the model at the beginning of the experiment because it is affected by the outer surface of the PCM packet that experienced a delayed onset time of melting compared to the inner surface.

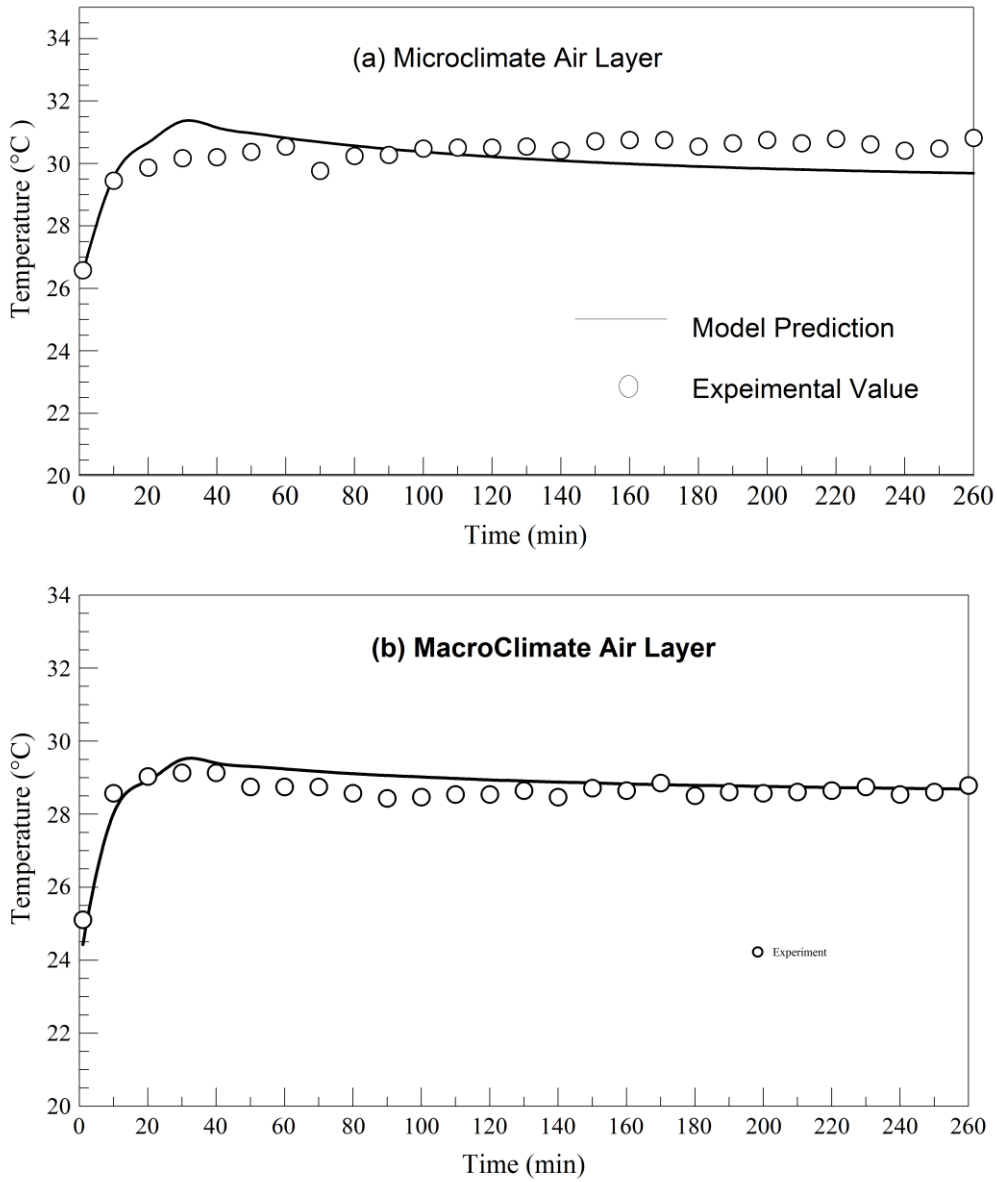


Figure 4: Plots of the averaged experimental readings and the model predictions of (a) the microclimate air layer temperature and (b) the macroclimate air layer temperature during the melting phase.

Figure 5 shows the experimental temperatures and the model predictions of the (a) microclimate air layer adjacent to (PCM-1) and microclimate air layer adjacent to (PCM-2) and (b) macroclimate air temperature. Good agreement exists between the measured and predicted

temperature profiles of the different air layers. It is clear that the two microclimate air layers have different temperatures before the PCM starts melting however, as the melting phase starts, these two layers reach almost the same temperature as would be expected after a period of time when initial conditions effect becomes insignificant. The maximum error attained for both microclimate air layers was about $\pm 8.5\%$. as for the macroclimate air layer temperature, the maximum error attained was 7.5%.

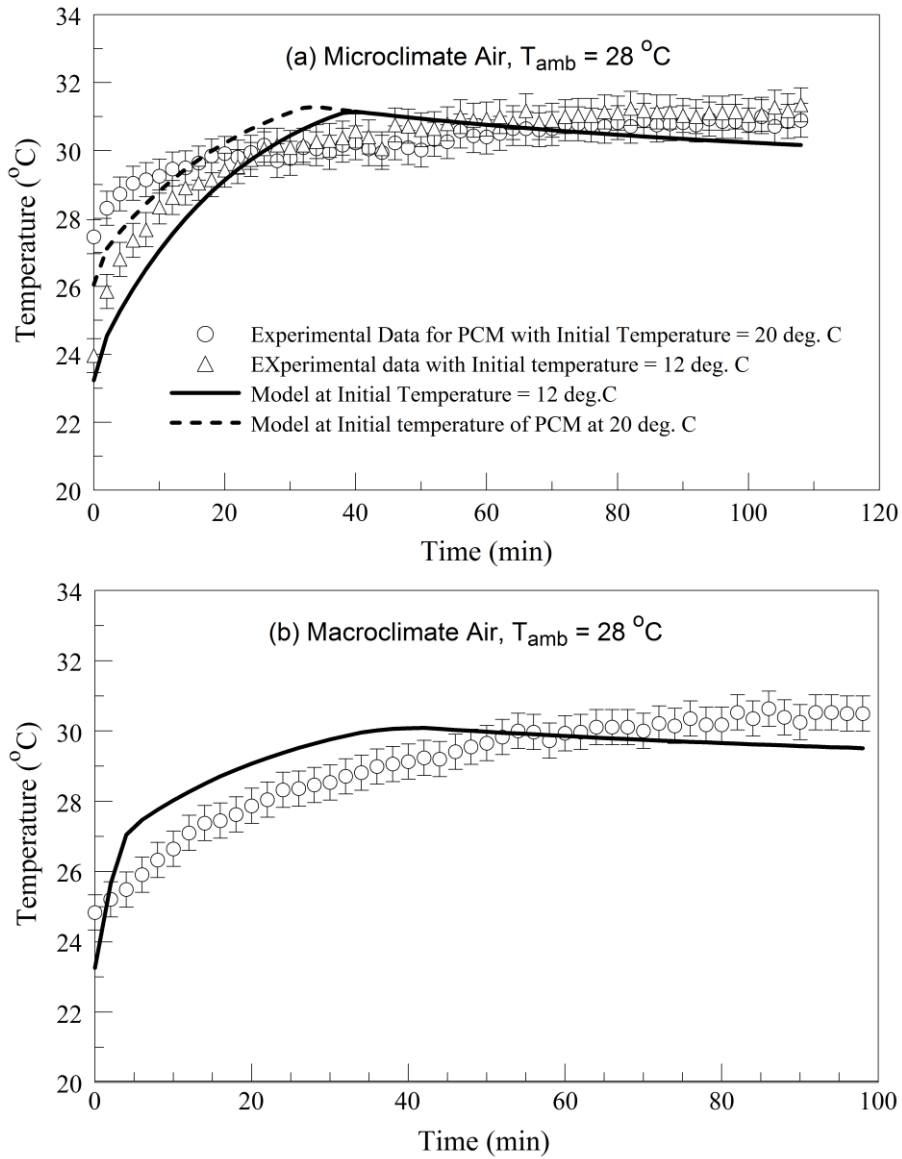


Figure 5: Plots of the averaged experimental readings and the model predictions of (a) the microclimate air layer temperatures adjacent to PCM(1) and PCM(2) and (b) the macroclimate air layer temperature during the melting phase.

2. Validation of the fabric-PCM model by published data

The temperature profile of the PCM predicted by the fabric-PCM model is validated by published experiment presented by Goa et al. [1]. In this paper an experiment is done on a

thermal manikin with constant skin temperature of 38°C placed in a chamber also at 38°C. The total area of the manikin is 1.77 m² and the torso is 0.57 m². The thermal manikin is dressed with clothing of 0.431 m²°C /W total insulation without the vest that is placed between a T-shirt and RB90 underwear firefighting ensemble. The cooling vest contained 21 PCM packets and its total weight was 1.973 kg. The covering area of the PCMs was 0.2054 m², which constituted 36% of the total area of the torso. The PCM was kept at 20°C overnight to solidify. The melting temperature of the PCMs was 32°C and the latent heat of fusion was 189.4 kJ/kg. The temperature of the inner and the outer surfaces of the PCM were measured and the average temperature was calculated [1]. In order to compare the experimental results and the predicted ones by the model, a simulation was performed at the exact experimental conditions published in Ref. [1]. Figure 6 shows the variation in time of the PCM temperature in the published experiment and the value predicted by the current fabric-PCM model demonstrating a good agreement between experimental and predicted values. The maximum errors between the model and the experimental results were 3.8%, 3% and 6 % with outer, average and inner PCM surface temperatures, respectively. Note that in the fabric-PCM model, the PCM is taken as lumped and this is why its temperature in the single phase is close to the average temperature of the experiment. The maximum error attained was ±0.3°C. However, in the melting phase, the model assumes a constant melting temperature of 32 °C throughout the melting process and this is why the PCM temperature in this phase is closer to the outer value with a maximum error of ±0.3°C.

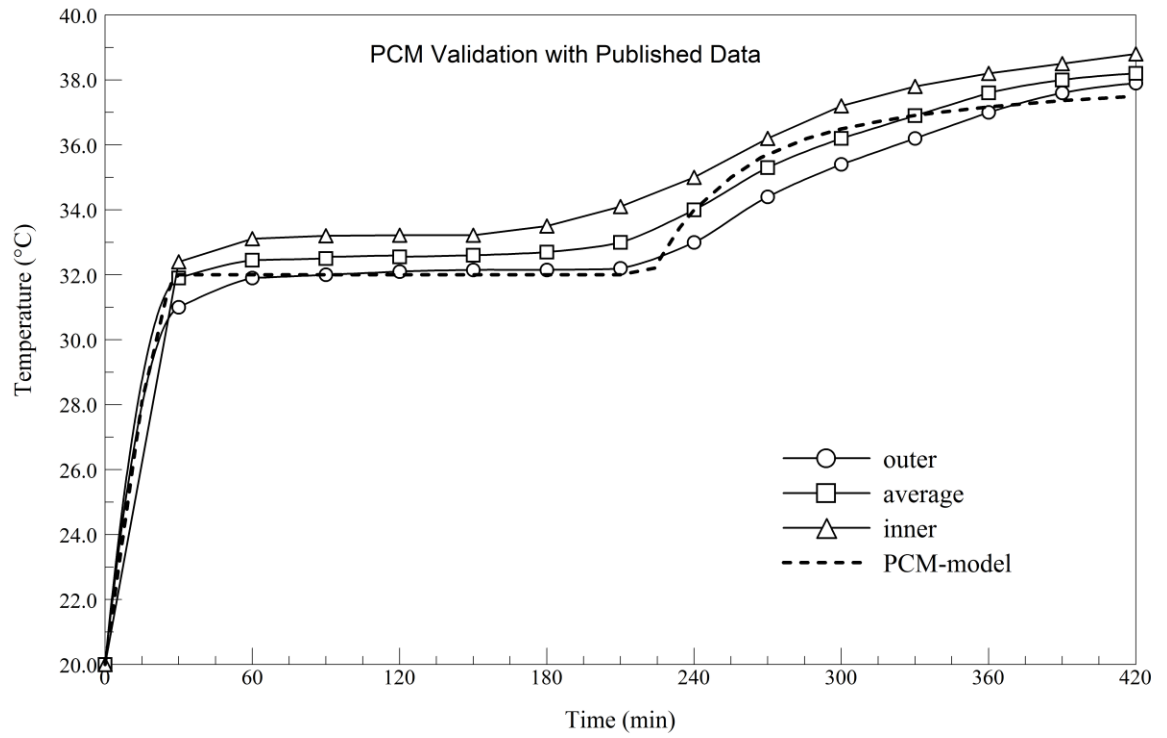


Figure 6: A plot of the variation in time of the PCM temperature in the published experiment [1] and the value predicted by the current fabric-PCM model.

CHAPTER III

INTEGRATION OF MATHEMATICAL MODEL WITH SEGMENTAL BIOHEAT MODEL

A. Introduction

In order to set more realistic boundary conditions for the fabric-PCM model, the transient bioheat model of Karaki et al. [28] is used. Their model is capable of predicting the instantaneous skin temperature of the different body segments. The bioheat model of Karaki et al. [28] divides the body into 31 segments including the division of the torso into eight segments; upper left chest, upper right chest, upper left back, upper right back, lower left chest, lower right chest, lower left back, lower right back [29]. Note that the upper torso has a larger surface area (0.402 m^2) than lower torso (0.246 m^2). This division of the torso into eight segments allowed variations in the skin temperature across the torso as well as the use of non-uniform environmental boundary conditions. These boundary conditions may include different exposure of each segment to ambient temperature, clothing, and different PCM packet properties. The fabric-PCM vest model is integrated with each of the eight torso segments and thus the number and the melting temperature of the PCM packets will be specified for each segment. When the PCM covering area does not match the area of the torso skin segment, the same segment skin temperature is used for parallel heat transfer paths into the fabric layer and the PCM-fabric layer while also accounting for radiation heat transfer [35-36]. At each time step, the skin temperature and the vapor pressure at the skin of the eight segments is calculated depending on the

microclimate air temperature predicted by the fabric-PCM vest model and assuming only water vapor transfer through the fabric and that the PCM is impermeable. Thus, the evolution of the instantaneous change of the state of the PCM directly affects the skin conditions and hence affects whole body response due to the continuous change in the medium surrounding it. Therefore, the total losses from the different parts from the human body and the torso in particular can be accurately predicted at each time step. The coupling methodology between the PCM vest model and the bioheat model in each time step is illustrated in figure 7.

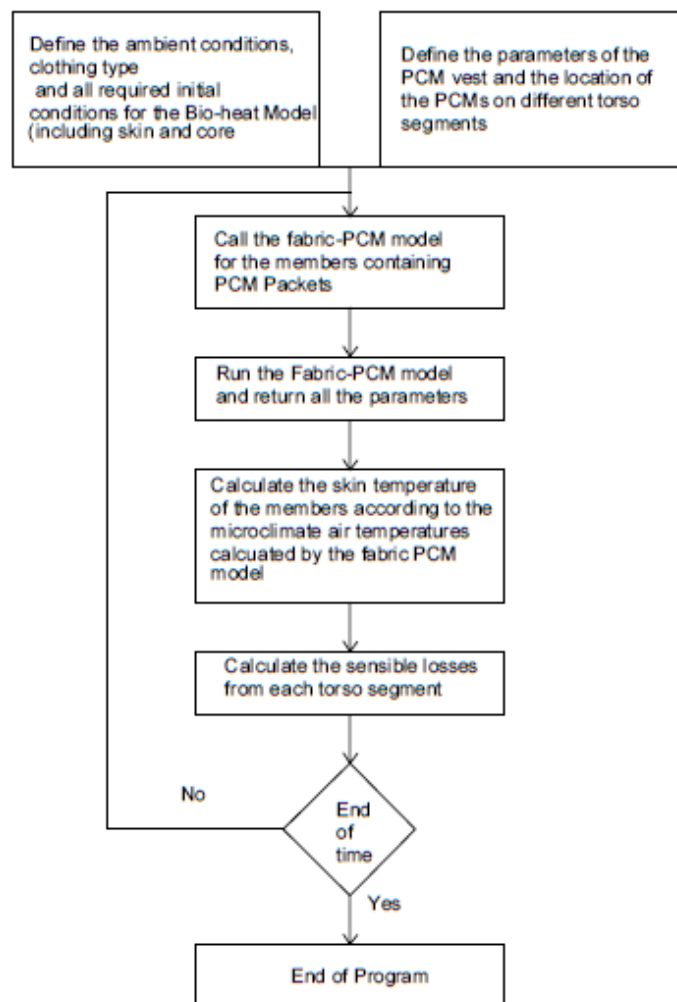


Figure 7: Flow chart of the integration of the fabric-PCM model with the Bio-heat Model

B. Validation of the integrated bio-heat model and the fabric PCM model

This section aims at validating the integrated bio-heat model with a published experiment by Chou et al on the effect of wearing cooling devices under protective clothing in a relatively hot environment [20]. This paper investigates the effectiveness of ice-packs (ICE) and PCM cooling vests by performing experiments on each type and comparing it against a no-cooling device (CON) case. This section presents the experimental results of the mean skin temperature and the core temperature in the (CON) and the PCM (20) cases published by Chou et al and compare it with simulation results from the bio-heat model. In the (CON) and PCM (20) cases, the subjects wore firefighting protective clothing of 1.53 clo and basic undergarments. The PCM (20) case included a cooling vest with 16 packs distributed on the chest and back. The melting temperature of the PCM used is 28°C and initially it was at 20°C. The latent and the specific heat are 35.1 cal/°C·g and 0.69 cal/°C·g respectively. The total surface area of the PCM packets is 1.792 cm². The average weight of the subjects is 62.5 kg and their maximum oxygen consumption is $V_{O_{2max}} = 45.8$ ml/min·kg. The total duration of the experiment was 50 minutes. For the first 10 minutes, the subjects rested in a pre-test room at 25 °C, 50%-60% relative humidity. Then they entered the test room where they rested for another 10 minutes at 30 °C, 50% relative humidity. Afterwards, they performed cycling on a bicycle ergometer for 30 minutes at 55% $V_{O_{2max}}$ followed by a 10 minutes recovery period. The simulations done on the bio-heat model took into consideration the experimental conditions. The rectal temperature was compared against the average core temperature predicted by the model. Moreover, the experimental skin temperature was compared against the average skin temperature calculated using DuBois's equation [37] similar to that used in the experiment. In the experiment the subjects faced a transition from resting to cycling during which their

metabolic rate increased. Thomas et al [38] studied the response of the oxygen uptake during the transition from rest to a steady exercise and proposed three stage exponential models that fit the oxygen uptake of four different work rates ranging from moderate to heavy. Therefore, the equation of the oxygen uptake for a moderate exercise proposed by [38], is converted to metabolic rate and is used in the bio-heat model to account for the gradual increase in the metabolic rate during the transition from rest to work.

Figure 8 shows the published experimental data and the model predictions of (a) the mean skin temperature and (b) the core temperature. The predicted values of the integrated bioheat model agree well with those measured by the experiment. The maximum error attained in the mean skin temperature is 0.75 °C at the recovery period for (CON) case and 0.64 °C for the (PCM-20) case. On the other hand, the maximum error attained for the core temperature is 0.3 °C for the (CON) case and 0.15 °C for the (PCM-20) case.

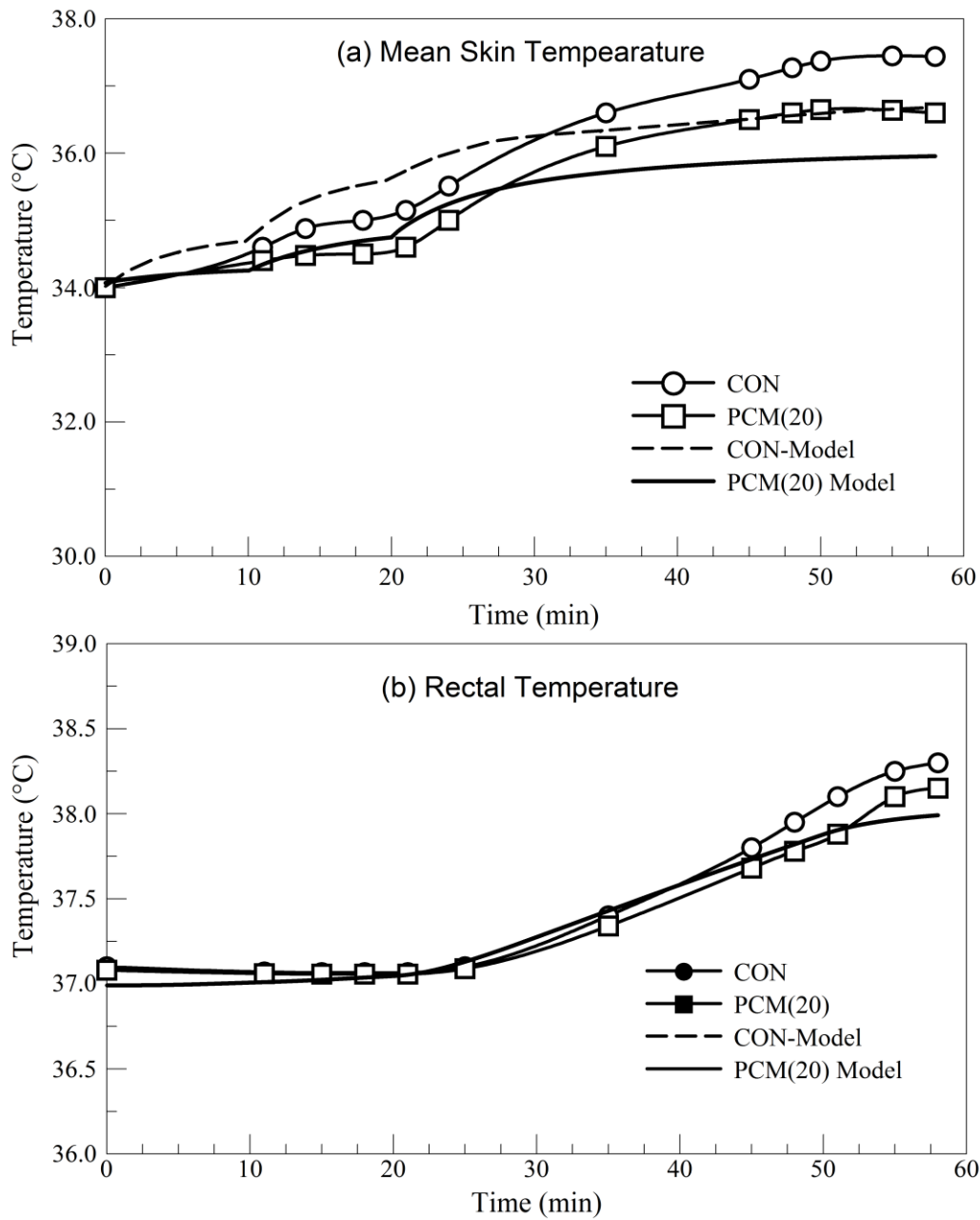


Figure 8: Plots of published experimental data [20] and the model predictions of (a) mean skin temperature and (b) rectal temperature for the case when PCM is present (PCM20) and for the case without the cooling device (CON).

C. Parametric Study using integrated bioheat model and Fabric-PCM model

The integrated fabric-PCM model and the bio-heat model are used to perform a parametric study to understand the effect of different physical parameters on the performance of the cooling vest. In this section, these parameters will be studied by conducting simulations under different conditions for a base case, where no PCM packets are used in the vest and with a PCM vest to compare body heat loss and torso skin temperature for all the cases. The parametric study aims to provide some recommendations on the best PCM melting temperature, PCM-vest's covering area and the distribution of the PCM packets on the vest covering the torso.

1. Effect of PCM melting temperature

The melting temperature of the phase change material is an important parameter to study because it directly influences the temperature of the microclimate air near the skin throughout the melting phase. Three melting temperatures will be investigated, 21°C, 24°C and 26°C. All PCMs are considered to have the same initial temperature, which is taken to be 20°C. These three cases will also be compared with the base-case scenario. The three vests contain the same number of PCM packets; the total cooling area is 0.22 m², which is 47% of the whole torso. Note that these packets are distributed equally among the eight parts of the torso, upper front right (UFR), upper front left (UFL), upper back right (UBR), upper back left (UBL), lower front right (LFR), lower front left (LFL), lower back right (LBR), lower back left (LBL). Therefore the upper and the lower torso have the same number of PCM packets. The four simulations are conducted at the same ambient conditions of temperature 32°C and 50% relative humidity.

Figure 9 shows the variation in time of the mean skin temperature of the torso for the base case without PCM and for PCM vest at three melting temperatures. It is clear that at the melting temperature of 21°C of the PCM vest, the skin temperature decreased by about 0.7°C.

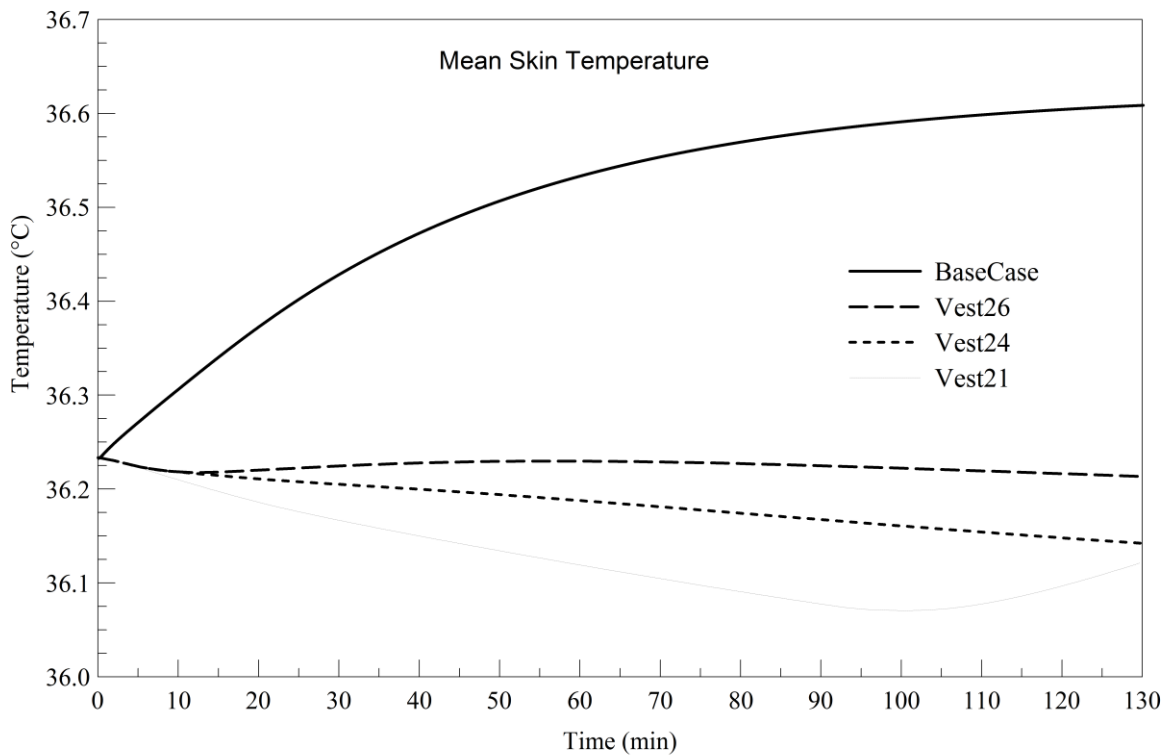


Figure 9: A plot of the variation in time of the mean skin temperature of the torso for the base case without PCM and for PCM vest at three melting temperatures.

The reduction in the skin temperature over time will be reflected on the sensible losses from the skin that are presented in figure. 10. The graph shows that the vest with PCM melting point of 24°C case results in a sudden increase in sensible losses at the beginning. This is due to the effect of the contact of the PCMs that are initially at low temperature of 20 °C that caused a temperature gradient between the skin and the microclimate air adjacent to it. The decrease in the

losses in the second stage, which is before the onset of melting, is due to the increase in the temperature of the PCM and thus the microclimate air. During melting, the skin temperature is decreasing and hence is increasing the gradient with the microclimate air that almost stabilized due to the constant melting temperature of the PCM. This has led to a slight increase of sensible heat losses during this period of the PCM change of phase.

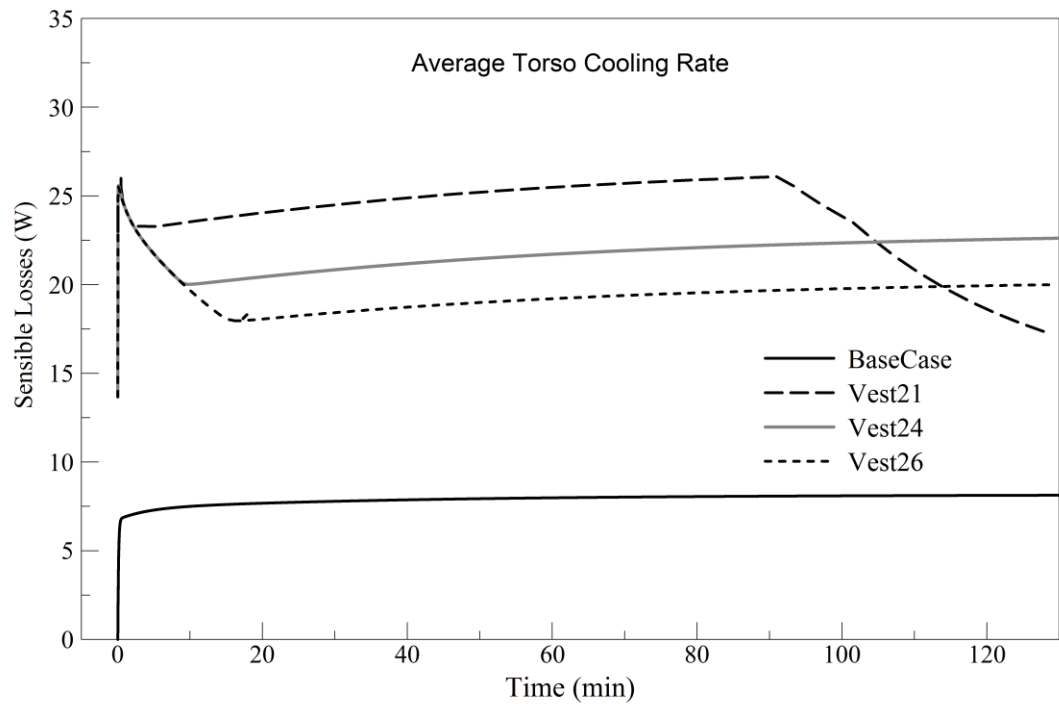


Figure 10: A plot of the variation in time of the sensible heat loss of the torso for the base case without PCM and for PCM vest at three melting temperatures.

Table 1 shows the onset of melting of the PCM, the total time for complete melting and the average sensible loss from the torso during the melting phase. It is clear that as the melting temperature increases, the time needed for the PCM to start melting is delayed and the total time

of melting is prolonged. As for the cooling rate, it is also clear that a larger cooling rate at lower melting temperature. It can be deduced from this comparison that when a faster cooling effect is needed, a lower melting temperature is desirable, however, for a prolonged cooling duration, a higher melting temperature is recommended.

| Case | Initial Temperature of PCM (°C) | Melting Temperature (°C) | Onset of melting (min) | Total time of melting (min) | Average Cooling Rate (W) |
|--------|---------------------------------|--------------------------|------------------------|-----------------------------|--------------------------|
| Vest21 | 20 | 21 | 1.7 | 1.5 | 25 |
| Vest24 | 20 | 24 | 8.9 | 2 | 21.7 |
| Vest26 | 20 | 26 | 15 | 3 | 19.5 |

Table 1: Comparison of Onset of melting, cooling duration and average sensible losses from torso during the melting phase between Vest21, Vest24 and Vest26

2. Effect of the cooling vest covering area by the PCM

In this section the effect of the covering area of the PCMs will be studied. In order to evaluate this parameter, two vest prototypes are compared: one with a total covering area of 47% (CV47%) of the torso and another with a total covering area of 23% (CV23%) for two melting temperatures (24 °C and 21 °C). The upper and the lower torso parts have the same number of PCM packets. All PCMs are considered to have the same initial temperature, which is taken to be 20 °C. For both melting temperatures, the simulations addressing different covering areas are done in ambient conditions of 32°C and 50% relative humidity. Note that the two vests identical PCM packets; i.e., identical sizes and mass. Table 2 shows that the onset of melting is not affected but the total time of melting is reduced when the covering area decreases. Moreover, the sensible loss from the torso during melting is also reduced.

| Case | Initial Temperature of PCM (°C) | Onset of melting (min) | Total time of melting (hrs) | Average Cooling Rate (W) |
|------------|---------------------------------|------------------------|-----------------------------|--------------------------|
| CV23%_Tm24 | 20 | 8.2 | 1.7 | 16.7 |
| CV47%_Tm24 | 20 | 8.9 | 2 | 21.7 |
| CV23%_Tm21 | 20 | 1.8 | 1.32 | 18.42 |
| CV47%_Tm21 | 20 | 1.7 | 1.5 | 25 |

Table 2: Comparison between 23% and 47% of PCM covering area of the torso

3. Effect of the mass of the PCM

The mass of the phase change material also has an effect on the effectiveness of the cooling vest. For this reason, two cases are studied where the two vests have the same total covering area but different weights. The weight of Vest-A is 0.88 Kg while that of Vest-B is 1.7 Kg. The two vests have the same melting temperature of 21 °C at initial temperature of 20 °C while the PCM packets are covering 23% of the area of the torso. From table 3, it is clear that the mass of the cooling vest has a direct effect on the cooling duration of the vest and did not have an effect on the cooling rate.

| Case | Mass (Kg) | Initial Temperature of PCM (°) | Onset of melting (mins) | Total Time of Melting (mins) | Average Cooling Rate (W) |
|--------|-----------|--------------------------------|-------------------------|------------------------------|--------------------------|
| Vest-A | 0.88 | 20 | 1.8 | 79.2 | 18.42 |
| Vest-B | 1.76 | 20 | 3.65 | 162 | 19.17 |

Table 3: Comparison between two Vests of different Mass

4. Effect of the location of the PCM

As mentioned earlier, the bio-heat model used in this work divides the torso into eight parts where the upper and the lower segments have different skin temperatures and areas. In this section, the effectiveness of placing the PCM packets on both or either of the upper and the lower parts of the torso will be assessed in comparison with the no PCM case.

Simulations were performed for thirteen cooling vest cases with different PCM locations, mass, thickness and melting points in the upper and lower trunk segments as presented in table 4.

| Case | T_{melting} (°C) | Total Area of PCMs on Upper Torso (m ²) | Total Area of PCMs on Lower Torso (m ²) | Thickness of PCM on Upper Torso (m) | Thickness of PCM on Lower Torso (m) | Mass of PCM on Upper Torso (Kg) | Mass of PCM on Lower Torso (Kg) | Total Mass of PCM (Kg) |
|-------------------------------|---------------------------|---|---|-------------------------------------|-------------------------------------|---------------------------------|---------------------------------|------------------------|
| Vest21 | 21 | 0.16 | 0.16 | 0.002 | 0.002 | 0.88 | 0.88 | 1.76 |
| Vest24 | 24 | 0.16 | 0.16 | 0.002 | 0.002 | 0.88 | 0.88 | 1.76 |
| Vest26 | 26 | 0.16 | 0.16 | 0.002 | 0.002 | 0.88 | 0.88 | 1.76 |
| Non-Uniform-Vest24 | 24 | 0.12 | 0.07 | 0.002 | 0.002 | 0.66 | 0.44 | 1.1 |
| Upper-Only-PCM-Vest24-0.88Kg | 24 | 0.16 | 0 | 0.002 | 0.002 | 0.88 | 0 | 0.88 |
| Lower-Only-PCM-Vest24-0.88Kg | 24 | 0 | 0.16 | 0.002 | 0.002 | 0 | 0.88 | 0.88 |
| Thick PCM on Upper Torso-Vest | 21 | 0.07 | 0.16 | 0.004 | 0.002 | 0.88 | 0.88 | 1.76 |

| | | | | | | | | |
|--------------------------------------|----|------|------|-------|-------|------|------|------|
| Thick PCM on Lower Torso-Vest | 21 | 0.16 | 0.07 | 0.002 | 0.004 | 0.88 | 0.88 | 1.76 |
| Upper Only-PCM, Vest t21-1.76Kg | 21 | 0.31 | 0 | 0.002 | 0.002 | 1.76 | 0 | 1.76 |
| Lower – Only-PCM, Vest t21-1.76Kg | 21 | 0 | 0.31 | 0.002 | 0.002 | 0 | 1.76 | 1.76 |
| 75% Upper, 25% Lower Vest t21-1.76Kg | 21 | 0.23 | 0.07 | 0.002 | 0.002 | 1.32 | 0.44 | 1.76 |
| 25% Upper, 75% Lower Vest t21-1.76Kg | 21 | 0.07 | 0.23 | 0.002 | 0.002 | 0.44 | 1.32 | 1.76 |

Table 4: Characteristic of different cooling vest cases

The onset of melting, total melting duration, sensible losses and cooling rate of the upper and the lower torso segments are presented in Table 5. It is clear that for all melting temperatures (Vest21, Vest24 and Vest26), the PCMs located on the upper torso melted earlier and had a shorter melting duration than those located on the lower torso. This is because of smaller PCM covering area of the upper torso segment compared to the lower torso PCM covering area resulting in higher skin temperature and leading to higher microclimate air temperature. Moreover, the sensible losses and the average cooling rate during the melting phase from the upper torso were greater than the lower torso. On the other hand, in the Non-Uniform-Vest24, where there is non-uniformity in the number of PCMs present on the upper and lower

torso while having the same PCM covering area of both segments, it was shown that the PCMs on both parts had the same melting duration with higher losses from the upper torso.

| Case | Torso Segment | Onset of melting (min) | Total Melting Duration (min) | Sensible Losses (kJ) | Total Sensible Losses (kJ) | Average Cooling Rate (W) | Mean skin temp | Mean skin temp of torso |
|-------------------------------|---------------|------------------------|------------------------------|----------------------|----------------------------|--------------------------|----------------|-------------------------|
| Base-Case | Upper | - | - | - | - | 6.10 | 36.45 | 36.61 |
| | Lower | - | - | - | | 4.31 | 36.77 | |
| Vest21 | Upper | 1.98 | 89.37 | 75.60 | 141.60 | 13.90 | 35.80 | 35.95 |
| | Lower | 2.12 | 99.32 | 66.00 | | 11.07 | 36.10 | |
| Vest24 | Upper | 9.00 | 121.33 | 93.50 | 171.60 | 12.16 | 35.90 | 36.09 |
| | Lower | 9.65 | 136.08 | 78.10 | | 8.65 | 36.27 | |
| Vest26 | Upper | 15.00 | 157.88 | 104.00 | 195.26 | 10.95 | 36.00 | 36.19 |
| | Lower | 16.35 | 177.53 | 91.26 | | 8.57 | 36.38 | |
| Non-Uniform-Vest24 | Upper | 8.56 | 113.63 | 74.18 | 124.23 | 10.80 | 36.00 | 36.20 |
| | Lower | 8.56 | 113.00 | 50.05 | | 7.40 | 36.40 | |
| Upper Only-PCM Vest24-0.88Kg | Upper | 8.90 | 121.00 | 89.00 | 121.80 | 12.00 | 36.00 | 36.40 |
| | Lower | 0.00 | 0.00 | 33.80 | | - | 36.80 | |
| Lower Only-PCM Vest24-0.88Kg | Upper | 0.00 | 0.00 | 52.00 | 127.00 | - | 36.50 | 36.40 |
| | Lower | 9.65 | 135.00 | 75.00 | | 9.67 | 36.30 | |
| Thick PCM on Upper Torso-Vest | Upper | 3.65 | 162.00 | 104.60 | 170.40 | 10.70 | 36.00 | 36.09 |
| | Lower | 2.10 | 99.33 | 65.80 | | 11.00 | 36.17 | |

| | | | | | | | | |
|---|-------|------|--------|--------|--------|-------|-------|-------|
| Thick PCM on Lower Torso-Vest | Upper | 1.98 | 89.34 | 74.60 | 164.60 | 13.91 | 35.94 | 36.13 |
| | Lower | 3.78 | 173.40 | 90.00 | | 8.67 | 36.32 | |
| Upper - Only-PCM, Vest21 - 1.76Kg | Upper | 2.25 | 109.00 | 121.48 | 151.98 | 18.40 | 35.70 | 36.25 |
| | Lower | - | - | 30.50 | | 4.60 | 36.80 | |
| Lower - Only-PCM, Vest21 - 1.76Kg | Upper | - | - | 52.00 | 155.50 | 6.70 | 36.48 | 36.24 |
| | Lower | 2.50 | 126.00 | 103.50 | | 13.30 | 36.00 | |
| 75%Upper, 25%Lower OWE RVest 21- 1.76Kg | Upper | 2.10 | 97.85 | 74.00 | 105.70 | 12.60 | 36.20 | 36.40 |
| | Lower | 1.90 | 83.60 | 31.70 | | 6.30 | 36.60 | |
| 25%Upper, 75%Lower OWE RVest 21- 1.76Kg | Upper | 1.85 | 78.00 | 37.30 | 102.80 | 7.70 | 36.40 | 36.40 |
| | Lower | 2.30 | 113.68 | 65.50 | | 9.61 | 36.40 | |

Table 5: Comparison between the upper and the lower torso segments in different vest cases

The Upper-Only-PCM Vest24 and the Lower-Only-PCM Vest24 are vest prototypes with PCMs placed in the upper or in the lower torso segments. Placing the PCM on the upper torso is more effective in increasing torso cooling rate. Vest21, Thick PCM on Upper Torso-

Vest21 and Thick PCM on Lower Torso-Vest21 have identical mass distribution of PCMs on the upper and lower torso parts. Comparing between these three cases reveal that thicker PCMs have larger melting duration and sensible losses, it also shows that placing thicker PCMs on the upper torso gives highest total sensible losses from the torso.

In the last four vest prototypes, 1.76Kg of PCMs were distributed among the torso parts in four different ways. It is shown that placing all PCMs on the upper torso only provided higher cooling rate than placing it on the lower torso. The same result is shown when 75% of the PCM weight is placed on the upper torso in the (75% Upper, 25% LOWER Vest21-1.76Kg) case. Moreover, comparing (Upper –Only-PCM, Vest21-1.76Kg) and (Lower –Only-PCM, Vest21-1.76Kg) cases reveals that the sensible losses from the upper torso are greater than those released from the lower torso. This also can be deduced when comparing (75% Upper, 25% LOWER Vest21-1.76Kg) and (75% Lower, 25% Upper Vest21-1.76Kg) cases. Therefore for the same mass of PCM, the upper torso is responsible for higher sensible losses.

Comparing the all vest prototypes, it can be shown that placing 1.76Kg on the upper torso only (Upper – Only-PCM, Vest21-1.76Kg) gave the highest losses from the upper torso and the lowest upper torso skin temperature. However, the (Thick PCM on Upper Torso-Vest) vest case gave the highest total sensible losses from the torso.

The parametric simulation results reveal that a lower melting temperature is favored when fast cooling is needed. Moreover, the covering area affects the cooling rate while the mass of the PCM (thickness) affect the total duration of melting. These findings are similar to the experimental findings by Gao et al. [1]. It is also found that the upper torso is responsible for higher sensible losses than the lower torso even when the two segments have the same covering

areas. Therefore it is recommended to increase the PCMs on the upper torso while reducing them on the lower one.

CHAPTER IV

CONCLUSION

A mathematical model is developed and is validated by experiment to simulate heat and mass transfer in a cooling vest containing salt PCM packets. The model predictions of the air layers temperatures shows a good agreement with the experimental findings with slight differences due to the lumping assumption of the air layers and the PCM taken by the model. The temperature profile of the PCM is also validated with published data. This model is then integrated with a segmental bio-heat model to set accurate boundary conditions. This integration allows for an accurate simulation of a human wearing a PCM cooling vest and present in a hot environment by predicting the instantaneous physiological body responses. The integration between these two models is validated with published experiment done on humans wearing PCM vest.

The integration of fabric-PCM model with bio-heat model allows studying the effect of the PCM vest on the skin temperature and sensible losses from the torso. A simulation study is done to investigate the effect of different parameters such melting temperature, covering area and mass of the PCM on the performance of the vest. The bio-heat model used in this work allows the determination of the effect of the PCM on the upper and lower torso knowing that these two segments function differently and thus have different skin temperatures.

The integration of the Fabric-PCM model and the segmental bio-heat model is a valuable tool to predict the instantaneous response of the human body affected by the presence of PCMs on different parts of the torso. This can be used to optimize the weight of the vest yet maintaining its performance. Heat stress indices [39] may be used later as indicators to comfort and

enhancement in performance caused by the presence of the cooling vest. Moreover, thermal sensation and comfort models may be used to study the effect of different vest prototypes [40]. The available models in literature propose empirical relations for comfort that depend on the variation of the core and skin temperatures of different segments. However, these models take the torso as one segment without dividing it into several segments. This restricts the use of the local comfort models in this type of study but also signifies the importance of studying of comfort while considering non-equal skin temperature of torso segments.

BIBLIOGRAPHY

- [1] C. Gao, K. Kuklane and I. Holmér, Cooling vests with phase change material packs: the, *Ergonomics*,53 (2010) 716-723 2010, vol. 53, no. 5, pp. 716-723.
- [2] N. Ghaddar., K. Ghali, S. Chehaitly, Assessing thermal comfort of active people in transitional spaces in presence of air movement, *Energy and Buildings* 43 (2011) 2832-2842
- [3] J Webster, EJ Holland , G Sleivert , RM Laing & BE Niven, A light-weight cooling vest enhances performance of athletes in the heat, *Ergonomics* 48 (7) (2005) 821-837.
- [4] A. D. Flouris and S. S. Cheung, Design and Control Optimization of Microclimate Liquid Cooling systems underneath Protective Clothing, *Annals of Biomedical Engineering* 34 (3) (2006) 359–372
- [5] A. L. Furtado, B. N. Craig, Cooling Suits, Physiological Response, and Task Performance in Hot Environments for the Power Industry, *International Journal of Occupational Safety and Ergonomics (JOSE)* 13 (13) (2007) 227-239
- [6] S. A. Nunnely, Water Cooled Garmets: A review, *Space Life Sciences* 2 (1970) 335-360
- [7] J.K. Johonson, Evaluation of Four Portable Cooling Vests for Workers Wearing Gas Extraction coveralls in Hot Environments, MS Thesis, University of South Florida, 2013.
- [8] T. Y. Meng, Design of a Microclimate Ventilation System, BE Thesis,. University of Southern Queensland, 2007
- [9] M. J. Loumala, J. Oska, J. A. Salmi, V. Linnamo, I. Holmer, J. Smolander, B. Dugue, Adding a cooling vest during cycling improves performance in a warm and humid conditions, *Journal of thermal Biology* 37 (2012) 47-55.
- [10] H. Hasegawa, T. Takatori, T. Kamura, and M. Yamasaki, Wearing a cooling Jacket during Exercise Reduces thermal strain and Improves Endurance Exercise Performance in a Warm Environment, *Journal of Strength and Conditioning Research* 19 (1) (2005) 122-128
- [11] S.A. Arngrimsson, D.S. Petitt, M.G. Stueck, D.K. Jorgensen, K.J. Cureton, Cooling vest worn during active warm-up improves 5-km run performance n the heat, *J Appl Physiol*, 96 (2004) 1867-1874
- [12] J.R. House, H. C. Lunt, R. Taylor. The impact of a phase-change cooling vest on heat strain and the effect of different cooling pack melting temperature, *Eur J Appl Physiol* 113 (2013) 1223-1231
- [13] S. Mondal, Phase change materials for smart textiles-An overview, *Applied Thermal Engineering* 28 (2008) 1536-1550
- [14] K. Ghali, N. Ghaddar, J. Harathani, Experimental and numerical investigation of the effect of phase change materials on clothing during periodic ventilation, *Textile Res. J.*, 74 (3) (2004) 205-214
- [15] M. Tate, D. Forster, D.E. Mainwaring, Influence of Garment design on elite athlete

- cooling, *Sports technol* 1 (2-3) (2008) 117-124
- [16] C. Gao, K. Kulakne, F. Wang, I. Holmer, Personal cooling with phase change materials to improve thermal comfort from a heat wave perspective, *Indoor air* 22 (6) (2012) 523-530
- [17] T. Lango, R. Nesbakken, H. Faerevik, K. Holbo, J. Reitan, Y. Yavuz, R. Marvik, Cooling vest for improving surgeons' thermal comfort: A multidisciplinary design project, *Minimally Invasive Therapy* 18(1) (2009) 1-10
- [18] J. Choi, M. Kim, J. Lee, Alleviation of Heat strain by Cooling Different Bodey areas during Red Pepper Harvest Work at WBGT 33°C, *Industrial Health* 46 (2008) 620-628
- [19] G. Bartkowiak, A. Dabrowska, A. Marszalek, Analysis of Thermoregulation properties of PCM garmets on the basis of ergonomic test, *Textile Research Journal* 83(2) (2013) 148 – 159.
- [20] C. Chou, Y. Tochihara, T. Kim, Physiological and subjective responses to cooling devices on firefighting protective clothing., *European Journal of Applied Physiology* 104 (2) (2008) 369-374
- [21] R. E. Reinertsen, H. Fårevik and K. Holbó, Optimizing the Performance of Phase-Change Materials in Personal Protective Clothing Systems, *International Journal of Occupational Safety and Ergonomics (JOSE)* 14 (1) (2008) 43–53.
- [22] W. Bendkowska, M. Kłonowska, K. Kopias and A. Bogdan, Thermal manikin evaluation of pcm cooling vests, *Fibres & Textiles in Eastern Europe* 18 (1) (2010) 70-74.
- [23] C. Gao, K. Kuklane, I. Holmér, Cooling effect of a PCM vest on a thermal manikin and on humans exposed to heat, *12th International Conference on Environmental Ergonomics In Environmental Ergonomics*, 12 (4) (2007) 146-149
- [24] C. Gao, K. Kulkane, I. Holmer, Cooling vests with phase change materials: the effect of melting temperature on heat strain alleviation in an extremely hot environment, *Eur J Appl Physiol* (111) (2011)1207-1216.
- [25] M. Zhao, C. Gao, F. Wang, K. Kulkane, I. Holmer, The torso cooling of vests incorporated with Phase Change Materials (PCMs): A Sweat Evaporation Perspective, *Textile Research*, 83 (4) 2013, 418-425
- [26] Q. Yifen, J. Nan, W. Weia, Z. Guangweia, X. Baoliang, Heat Transfer of Heat Sinking Vest with Phase-change Material, *Chinese Journal of Aeronautics* 24(6) (2011) 720–725.
- [27] M. Salloum, N. Ghaddar , K. Ghali, A new transient bio-heat model of the human body and its integration to clothing models. *International Journal of Thermal Science*, 46 (4) (2007) 371-384.
- [28] W. Karaki, N. Ghaddar, K. Ghali, K. Kaleve, I. Holmer, L. Leif. Vanguard, Human thermal response with improved AVA modeling of the digits. *International Journal of Thermal Sciences*, 67 (2013) 41-52.
- [29] K. Ghali, M. Othmani, B. Jreije, N. Ghaddar, Simplified Heat Transport Model of a Wind-permeable Clothed Cylinder Subject to Swinging Motion, *Textile Research Journal*

- 79 (11) (2009) 1043-1055
- [30] A. Bejan, Convection Heat Transfer, 2nd Edition, Wiley-Interscience, 1994.
(ISBN: 0471579726)
- [31] W.E. Mortan, L.W. Hearle., Physical Properties of Textile Fibers. London: Heinemann, 1975.
- [32] R.W. Hyland, A. Wexler, Formulations for the thermo- dynamic properties of the saturated phases of H₂O from 173.15 K to 473.15 K., ASHRAE Trans. 89 (1983) 500–519.
- [33] <http://swedeproducts.se/econtent/166>
- [34] N. Ghaddar, K. Ghali, J. Harathani, E. Jaroudi, Ventilation rates of micro-climate air annulus of the clothing-skin system under periodic motion, International Journal of Heat and Mass Transfer 48(15) (2005) 3151-3166.
- [35] W. Lotens, Heat Transfer from Humans Wearing Clothing, Doctoral Thesis, TNO Institute for Perception, Soesterberg, The Netherlands, 1993.
- [36] K. Ghali, M. Al-Othmani, B. Jreije, N. Ghaddar, Simplified heat transport model of wind-permeable clothed cylinder subject to swinging motion. Textile Research Journal, 79 (11) (2009) 1043-1055.
- [37] J.D. Hardy, E.F. Dubois, The Technique of measuring radiation and convection, Journal of Nutrition 15 (1938) 461-475.
- [38] J. B. Thomas, A. M. Paul, Linear and non linear characteristics of oxygen uptake kinetics during heavy exercise, The American Physiological Society 71 (1991) 2099-2106.
- [39] S. M. Daniel, A. Shitzer, K. B. Pandolf, A physiological strain index to evaluate heat stress, Am. J. Physiol. 275 (Regulatory Integrative Comp. Physiol. 44) (1998) R129-R134.
- [40] H.Zhang, Human Thermal Sensation and Comfort in Transient and Non-Uniform Thermal Environments, Doctoral Thesis, University of California, Berkeley, 2003.